The Journal of Experimental Biology 215, 584-589

doi:10.1242/jeb.066019

A novel function for a carotenoid: astaxanthin used as a polarizer for visual signalling in a mantis shrimp

Tsyr-Huei Chiou[1,2,*], Allen R. Place[3], Roy L. Caldwell[4], N. Justin Marshall[2] and Thomas W. Cronin[1]

[1]Department of Biological Sciences, University of Maryland Baltimore County, Baltimore, MD 21250, USA, [2]Queensland Brain Institute, The University of Queensland, Brisbane, QLD 4072, Australia, [3]Center of Marine Biotechnology, University of Maryland Biotechnology Institute, Baltimore, MD 21202, USA and [4]Department of Integrative Biology, University of California, Berkeley, CA 94720, USA

*Author for correspondence (t.chiou@uq.edu.au)

Accepted 17 November 2011

SUMMARY

Biological signals based on color patterns are well known, but some animals communicate by producing patterns of polarized light. Known biological polarizers are all based on physical interactions with light such as birefringence, differential reflection or scattering. We describe a novel biological polarizer in a marine crustacean based on linear dichroism of a carotenoid molecule. The red-colored, dichroic ketocarotenoid pigment astaxanthin is deposited in the antennal scale of a stomatopod crustacean, *Odontodactylus scyllarus*. Positive correlation between partial polarization and the presence of astaxanthin indicates that the antennal scale polarizes light with astaxanthin. Both the optical properties and the fine structure of the polarizationally active cuticle suggest that the dipole axes of the astaxanthin molecules are oriented nearly normal to the surface of the antennal scale. While dichroic retinoids are used as visual pigment chromophores to absorb and detect polarized light, this is the first demonstration of the use of a carotenoid to produce a polarizing signal. By using the intrinsic dichroism of the carotenoid molecule and orienting the molecule in tissue, nature has engineered a previously undescribed form of biological polarizer.

Key words: stomatopod, polarized light, carotenoid, astaxanthin, linear dichroism

INTRODUCTION

Consider light as a form of electromagnetic radiation. As each photon of light propagates, its electric field vibrates like a wave. The axis of vibration is thus called the electric field vector angle, or more commonly e-vector angle. If the majority of the photons in a beam of light have nearly parallel e-vectors, the resulting beam of light is said to be linearly polarized (Feynman et al., 1963). The use of color patterns for visual signaling has long been recognized, but recent work reveals that some animals can communicate by displaying patterns of polarized light (Boal et al., 2004; Chiou et al., 2011; Cronin et al., 2003b; Mäthger and Hanlon, 2006; Sweeney et al., 2003). As stomatopod crustaceans are equipped with a visual system that is highly specialized and capable of multi-axis analysis of polarized light, they are well adapted for detecting and analyzing polarization signals (Chiou et al., 2008; Cronin et al., 2003b; Marshall et al., 1999).

Like other stomatopod crustaceans, *Odontodactylus scyllarus* (Linnaeus 1758) possess a pair of thin and flattened antennal scales, connected to the bases of the antennae with a flexible joint, and from which they extend out laterally. Typically, one side normally faces ventrally and anteriorly (the 'front side') and the other dorsally and posteriorly (the 'back side'; Fig. 1A). The back side of these planar, paddle-shaped structures is known to produce polarized light reflections (Chiou et al., 2005; Cronin et al., 2003a; Marshall et al., 1999).

Polarized-light-based body patterns have been found in a variety of animal groups, such as cephalopods, arthropods and vertebrates (Chiou et al., 2007; Denton et al., 1965; Horvath and Varju, 2003; Sweeney et al., 2003), where they frequently serve a role in communication, such as in mate choice or sexual recognition (Chiou et al., 2011; Sweeney et al., 2003). In *O. scyllarus*, the polarized antennal scale is thought to act as a visual signal (T.-H.C., R.L.C., N.J.M. and T.W.C., unpublished observations).

In previously described cases, biological polarizers are based on various types of physical interactions with light such as birefringence, differential reflection or scattering (Horvath and Varju, 2003; Parker, 2000; Shurcliff and Ballard, 1964). By contrast, the most common type of artificial polarizer, which can be found in optical laboratories as well as many consumer products (e.g. polarization sunglasses), is the dichroic polarizer. In such a device, the intrinsic dichroism of a pigment molecule causes incident nonpolarized light of a certain e-vector angle to be preferentially absorbed while the rest passes through – thus polarizing the light. The best-known dichroic molecules found in animals are visual pigments. The dichroic property of the retinal chromophore of visual pigments is the basis for polarization vision (Laughlin et al., 1975; Rossel, 1989; Snyder and Laughlin, 1975). Retinal, as well as many carotenoids, is intrinsically dichroic owing to its elongated polyene chain structures (Dolan et al., 2001; Hofrichter and Eaton, 1976; Margulies et al., 1985; Sperling and Rafferty, 1969). In fact, linear dichroism has been used to study the orientation of various carotenoids in artificial membranes (Dolan et al., 2001; Gruszecki, 2004; Sujak et al., 2005). Although many biological molecules are linearly dichroic, no biological polarizer based on intrinsically dichroic molecules has been found to date.

The goal of the present study was to determine the mechanism behind the polarized light reflections found in the antennal scale of the stomatopod crustacean *O. scyllarus*. Based on the results of our pigment-extraction experiments, together with our measurements of the optical properties, histological structure and carotenoid content of the antennal scale, this paper provides the first example of a dichroic polarizer found in nature.

MATERIALS AND METHODS

Spectral and imaging polarimetry

Spectral measurements and images were acquired as previously described (Chiou et al., 2007). In short, an antennal scale was secured on a tilting table for precise angular manipulation. Samples were submersed in seawater and measured under diffuse white-light illumination. Sets of three spectra or images were taken, respectively, with a spectrometer (USB2000, OceanOptis, Dunedin, FL, USA) or a digital camera (C5050Z, Olympus America, Center Valley, PA, USA) from each viewing angle through a polarization filter oriented at 0, 45 and 90 deg. For measuring the cuticle in transmitted light, we constructed a miniature tilting table by using a small plastic Petri dish. A piece of white Teflon tape serving as a diffuser was taped to the bottom inside the dish. A needle protruding into the Petri dish from the side was mounted parallel to the bottom of the dish to allow manipulation of the sample from outside the Petri dish. For producing repeatable angular adjustments, the tip of the needle was flattened with a pair of pliers. Samples were secured on the tip of needle with superglue, and the Petri dish was filled with seawater and placed under a compound microscope for spectral measurements.

The partial polarization and e-vector angles of the light reflected from, or transmitted through, the sample were then calculated based on approaches commonly used to analyze polarized light (Wolff and Andreou, 1995). To demonstrate better the properties of the polarization of the sample, false-color images based on the imaging polarimetry results derived from reflected light were weighted by the average brightness of each pixel, whereas, in those based on transmitted light, the false colors used to encode the e-vector were further coded for degree of polarization by brightness.

Electron microscopy

Specimens were fixed with 2.5% glutaraldehyde in PEMS buffer overnight at 4°C, post fixed with 1% osmium tetroxide for 2 h on ice and embedded in Epon. Thin sections of 60 to 90 nm were stained with saturated uranyl acetate in a 1:1 (v/v) methanol:ethanol solution followed by high-pH lead citrate (Reynolds, 1963) and viewed in a JEM-1010 transmission electron microscope (Jeol, Tokyo, Japan) operating at 80 kV.

Time-course of pigment extraction

Cuticle samples from the back side (i.e. the polarized side) of a fresh antennal scale were washed in fresh water, and any adhering soft tissue was brushed off. After air drying, pieces of cuticle of known weight were submersed in pure acetone for 5 min, 10 min or overnight (>12 h) to extract the pigment. After extraction, the cuticles were rehydrated in artificial sea water for polarization and absorbance spectra measurements. The absorbance of the pigment–acetone solutions was measured with a spectrophotometer (U-3010, Hitachi High Technologies America, San Jose, CA, USA) from 750 to 300 nm, with a sampling interval of 0.5 nm. Owing to the unavoidable removal of soft tissue, the polarization spectra of the pigment-extracted cuticle were measured using transmitted light with a 45 deg tilting angle.

High-performance liquid chiral chromatography

Synthetic astaxanthin (racemic mixture of all three stereoisomers) was obtained from Dr Ehrenstorfer, Augsburg, Germany. All solvents (Burdick and Jackson) as well as the phosphoric acid (85%) were HPLC grade. Lyophilized stomatopod parts were macerated with a mortar and pestle for 5 min and extracted with ethyl acetate or acetone until they were colorless. The extracts were centrifuged at 5500 ***g*** for 5 min followed by solvent evaporation under vacuum. The pigments were dissolved in a known volume of ethyl acetate or acetone prior to injection into the HPLC device. Pigment spectral analyses were performed on an Agilent 1100 HPLC attached to an Agilent Diode Array Detector (DAD, model #G1315B, Agilent Technologies, Santa Clara, CA, USA) with a micro high-pressure flow cell (G1315B#020; 6 mm path-length, 1.7 ml volume) over the wavelength range 190 to 700 nm. The entire UV–visible spectra were saved for all detectable peaks. Successful separation of the stereoisomers of astaxanthin (Grewe et al., 2007) was performed with a Chiralcel OD-RH column (5 μm, 150×4.6 mm i.d.) from Daicel (Tokyo, Japan) using 99:1 acetonitrile:phosphoric acid (3.5 mmol l^{-1}) at a flow rate of 0.25 ml min^{-1} under isocratic conditions and a temperature of 25°C.

Mathematical model for predicting partial polarization

To predict the polarization spectra of astaxanthin molecules that are aligned at a particular angle to the light source, we assume that the partial polarization is positively correlated with the effective length of the dipole moments of these aligned molecules For a dichroic molecule oriented in a beam of light, a cosine function for the angle between the dipole axis and the light source represents the effective relative length of the dipole axis. Consequently, we predict the transmitted polarization spectra $P(\lambda)$ of a group of aligned astaxanthin pigments, tilted at various angles, using a cosine function:

$$P(\lambda)=A(\lambda)\cos(\theta), \quad (1),$$

where $A(\lambda)$ is the absorption spectrum of pure astaxanthin in an acetone solution and θ represents the relative dipole axes of the astaxanthin molecules that we selected to match those of our experiments.

RESULTS

In the antennal scale of *O. scyllarus*, the degree of polarization observed in reflected light varies with the viewing angle (θ, defined as the angle between the direction of observation and the surface normal of the antennal scale). Spectral polarimetric measurements show this quantitatively (Fig. 1B). Thus, increasing the viewing angle from 0 to 60 deg along the short axis of the antennal scale elevates the degree of polarization from below 5% to over 90% (Fig. 1B). In addition, with increasing viewing angle, we found that the peaks of polarization spectra broadened and shifted towards longer wavelengths. However, the spectral range remains almost unchanged throughout all measured viewing angles (Fig. 1B). By contrast, when viewed from any fixed viewing angle, both partial polarization and the e-vector angle of the reflected light do not change with the rotation (i.e. the azimuth angle) of the antennal scale (Fig. 1C, θ=45 deg).

Sections across the thickness of the scale show that it contains a central region composed of soft tissue sandwiched between the hard exoskeletal tissues of the cuticle (Fig. 2A). The front and back sides of the cuticle have a distinctive red-colored layer. Viewing a section of the antennal scale through crossed polarizers in a polarizing microscope reveals that only the endocuticle layer of the back side of the antennal scale is polarization active (PA; Fig. 2A). Imaging polarimetry shows a distinctively high degree of polarization in the PA region in comparison with the rest of the cuticle (Fig. 2B), whereas the e-vector angle of the transmitted polarized light is always parallel to the surface of the antennal scale (Fig. 2C). Transmission electron microscopic images show that multilayer structures of various spatial frequencies are present in the PA cuticle layers of the antennal scale (Fig. 2D). From near the soft tissue

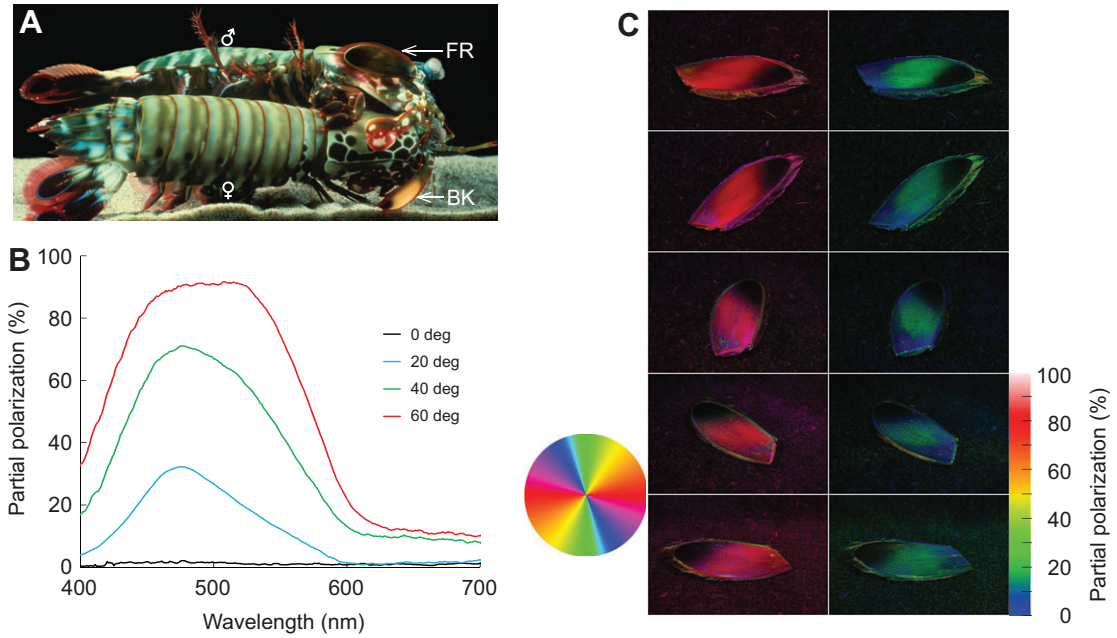

Fig. 1. Relationships between the viewing angle and the polarization properties of the antennal scale. (A) A mating pair of *O. scyllarus*, with the male showing front (FR) and the female showing the back (BK) sides of their right antennal scales. (B) The polarization spectra of the antennal scale. Each spectrum was calculated from sets of reflectance spectra obtained from an antennal scale measured through a linear polarizer rotated at three different angles, while being measured from a particular viewing angle, as indicated in the figure. (C) Imaging polarimetry showing the color-coded e-vector angle (left column) and color-coded partial polarization (right column) of the antennal scale, taken from a fixed 45 deg viewing angle. The color key for coding the e-vector angle is shown at the lower left, and the coding for partial polarization is at the lower right of the figure.

towards the surface, the spatial frequencies of the electron-dense layers in the cuticle gradually decrease from more than 10 layers per micrometre to less than one (Fig. 2D).

Because the polarization spectra and the coloration of the polarizationally active antennal scale are fairly close to the absorbance spectra of known carotenoids, we set out to look for the relationships between these pigments and the observed polarization properties of the antennal scale. Color variations between different layers visible in the cross-section of the antennal scale (Fig. 2A) suggest that pigments might occur not

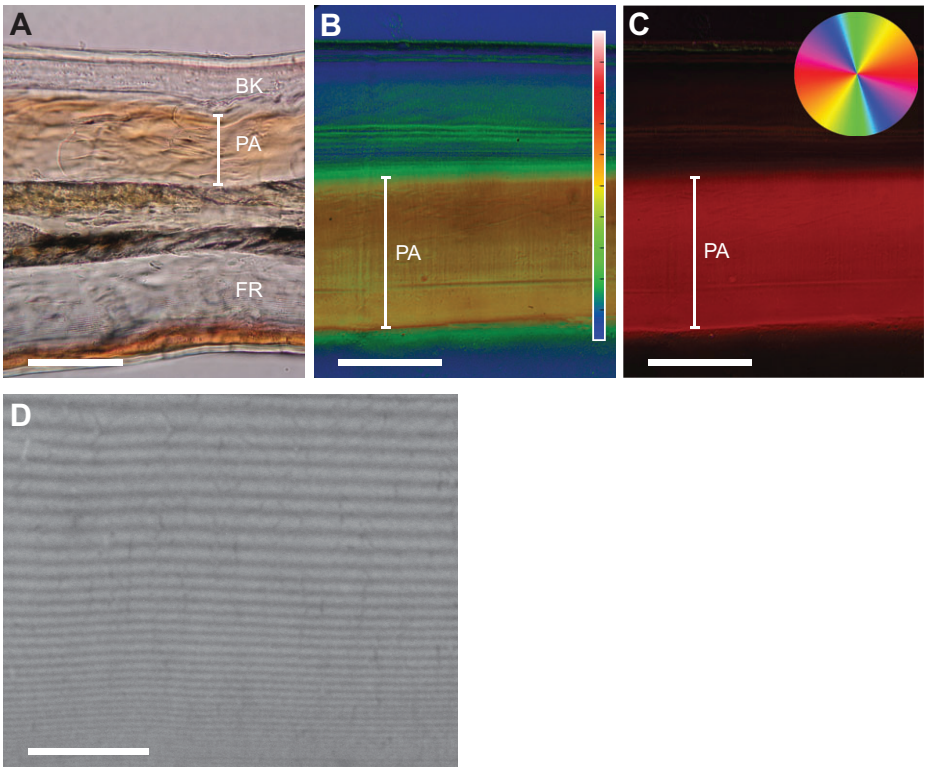

Fig. 2. The structure of the antennal scale of *O. scyllarus*. (A) Cross-section of the antennal scale viewed in a light microscope showing the natural color to indicate the potential location of pigments in different layers within the scale. 'Back side' (BK) marks the part of the antennal scale that is normally visible dorsally and posteriorly, whereas the 'front side' (FR) usually faces ventrally or anteriorly. The vertical bar marks the polarizationally active (PA) region in the section. Scale bar, 70 μm. (B,C) Imaging polarimetry showing the color-coded partial polarization (B) and e-vector angle (C) in a section of BK cuticle. The color key for coding of partial polarization is shown at the right of the image, with the same scale as in Fig. 1C. The color key for coding the e-vector angle is shown at the top right. Note that the brightness of the false-color image in (C) is scaled to the degree of polarization at each point. Scale bars, 50 μm. (D) High-magnification transmission electron micrograph showing the multilayer structures in the PA endocuticle layer of the antennal scale. Scale bar, 5 μm.

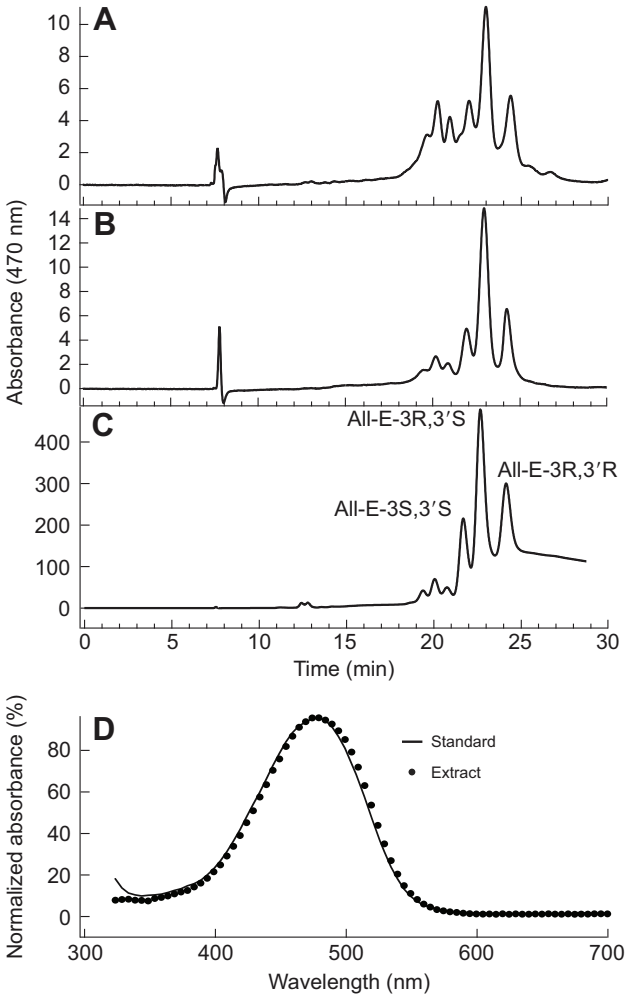

Fig. 3. The identity of the pigment extracted from the antennal scale of *O. scyllarus*. (A–C) High-performance liquid chiral chromatographic results showing the mixes of stereoisomers of the astaxanthin pigments extracted from the polarized back side of the antennal scale (A), the nonpolarized front side of the antennal scale (B) and from an astaxanthin standard consisting of a racemic mixture of the three possible stereoisomers (C). (D) Normalized absorption spectra of the astaxanthin standard in acetone (unbroken line) and the extract (black circles).

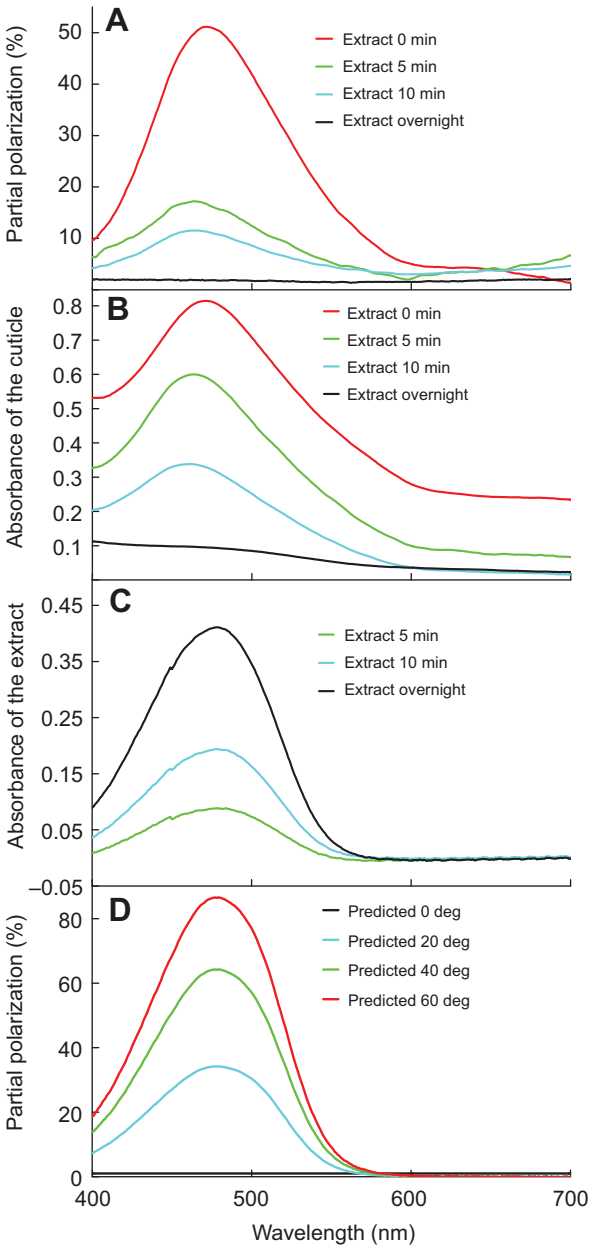

Fig. 4. Results of the time-course pigment-extraction experiment and predicted polarization spectra of an astaxanthin-based dichroic polarizer. Transmission polarization spectra of the antennal scale measured at θ=45 deg (A), absorbance spectra of the scale (B) and absorbance spectra of pigment extracts (C), showing the relationships between the time the sample is submersed in acetone and the remaining polarization (A), the remaining absorbance of the sample (B) and the absorbance (10 mm light path) of the acetone–extract solution (C). (D) Predicted polarization spectra of a dichroic polarizer, viewed at various angles, based on the absorbance spectrum of astaxanthin.

only in the optically active back half of the antennal scale but also in the front layers. We therefore analyzed both sides of the antennal scale for the identity of the pigments. By submersing the antennal scale in pure acetone, we found that the pigments within the cuticle can be easily extracted, resulting in a highly transparent cuticle. Based on absorption spectra and using high-performance liquid chiral chromatography, we found that the pigment in acetone extracts taken from either side of the antennal scale was indeed a carotenoid – the keto-carotenoid astaxanthin (Fig. 3). In the all-*trans* configuration, astaxanthin can exist in three possible stereoisomers: 3S,3′S, 3R,3′S or 3R,3′R, all of which have similar linear dichroism. As in the astaxanthin standard, all three of these stereoisomers exist in both samples at approximately the racemic ratio (1:2:1), which indicates that the astaxanthin in the antennal scale is itself a racemic mixture (Fig. 3).

When the pigment was gradually extracted from a sample of antennal scale cuticle by submersing it in acetone for increasing amounts of time, we found a strong negative relationship between the residual degree of partial polarization in the scale and the time the scale had been submersed in acetone (Fig. 4A). Similarly, as the characteristic astaxanthin absorbance of the antennal scales decreased, that of the extracts increased (Fig. 4B,C). Overnight extraction produced a highly transparent antennal scale (black trace in Fig. 4B) and completely abolished its polarization properties (black trace in Fig. 4A).

DISCUSSION

The predominant carotenoid pigment in the crustacean exoskeleton is astaxanthin (Goodwin and Srisukh, 1949; GoodWin, 1954; Matsuno et al., 1984; Zagalsky et al., 1990). When bound to specific proteins, thus forming astaxanthin–protein complexes, the absorbance spectra of the resulting carotenoproteins might be greatly shifted away from that of free astaxanthin (Zagalsky et al., 1990). The absorbance spectra of such carotenoproteins produce the colorful appearance of many crustaceans, including crabs and lobsters (Chayen et al., 2003). Similarly, incorporation of the ultraviolet-absorbing retinoid retinal into a diversity of opsin proteins can produce the variously absorbing visual pigments that underlie color vision (Okano et al., 1995; Yoshizawa, 1994). In this paper, we show that the dichroic properties of carotenoids can be used to produce polarized-light body reflections thought to be used in signaling.

In order to produce a polarizer within the antennal scale from astaxanthin, the pigment molecules within the antennal scale must have their dichroic axes aligned. Like other carotenoids, astaxanthin is generally located in cell membranes within the lipid bilayer. In this case, the relatively hydrophilic rings at each end of the molecule sit at the polar margins of the membrane, whereas the hydrophobic polyene chain extends through the lipid bilayer (Gruszecki, 2004). Although there is no apparent layering of the cell membrane in the polarizationally active cuticle, the layered structures of the antennal scale of *O. scyllarus* (Fig. 2D) could provide an organized framework for orienting astaxanthin pigments in the cuticle. Based on our polarization measurements (Fig. 1B,C), as well as the planes of the multilayer structure within the scale, the astaxanthin molecules must be oriented so that their dipole axes lie perpendicular to the surface of the antennal scale. This orientation is further supported by determining the transmission axis of the polarizationally active cuticle by using a polarization microscope (Fig. 2C). Consequently, the antennal scale transmits light equally at all e-vector angles when light arrives normal to the surface, but, as the scale tilts, it preferentially transmits light having its e-vector angle parallel to the surface of the scale. This explains why the e-vector angle of the reflected light is always parallel to the surface of the scale (Fig. 1C). The same polarization properties were observed on extracted BK cuticle under transmission illumination (Fig. 2C), which further supports the predicted orientation of astaxanthin molecules in the cuticle.

Acetone is a very powerful organic solvent, so submersion of the antennal scale in acetone might result in structural changes that cause the disappearance of the polarization. It is evident from our time-course pigment-extraction results (Fig. 4A,B) that the absorbance and the partial polarization of the cuticle are not linearly correlated. A likely cause of this is that submersion in acetone causes the axes of the astaxanthin pigments to become misaligned as they disperse out of their locations in the cuticle. As a result, the rate of the decrease in partial polarization is greater than that of the absorbance (Fig. 4A,B). The HPLC analysis suggests that, besides the astaxanthin, there is no other pigment present that could cause the observed changes in polarization properties.

Based on the absorption spectrum of pure astaxanthin (Fig. 3D) and the hypothesized arrangement of the molecule in the cuticle, we predicted the partial polarization of the resulting optics using simple cosine functions, as shown in Eqn 1. The predicted polarization spectra (Fig. 4D) are well matched to the experimental results (Fig. 1B). Note that the dipole axis of the astaxanthin in our hypothesized filter is perpendicular to the surface of the scale, so there is a 90 deg difference between tilt angle and the θ used in Eqn 1 to predict the curve. Because a dichroic polarizer acts in transmission, not reflection, the differences between predicted spectra and experimental results probably arise from additional polarization of light when it reflects from layers shallower or deeper in the cuticle, particularly as the angle of incidence approaches Brewster's angle. As is evident from measurements obtained in the transmission mode (Fig. 4A), at a 45 deg viewing angle, the peak of the partial polarization spectrum is identical to that of the absorbance spectrum of astaxanthin.

Our results show that the polarization reflections from the antennal scales of stomatopods are produced by the dichroic properties of astaxanthin molecules, oriented vertically within the antennal scale. Such an arrangement provides an elegant way for the animal to control the strength of its polarization signals, by orienting or changing the angle of the scale as desired, relative to the intended receiver. Behavioral observations indicate that one function of the antennal scale of *O. scyllarus* is similar to that of a submarine bow plane, acting to steer the animal in the pitch plane when swimming. *O. scyllarus*, and probably other species as well, have evolved an additional use for this appendage unrelated to its mechanical or hydrodynamic functions. By using a dichroic material within the antennal scale, it becomes capable of producing signals that vary with its orientation and are thus analogous to time-varying color signals – only here the changes are in polarization content instead of color. To our knowledge, this is the first time a biological polarizer based on dichroic molecules has been reported. As astaxanthin is widely distributed among crustaceans and other animals, it is likely that other animals use this or other carotenoid molecules in unusual ways.

ACKNOWLEDGEMENTS

We thank Dr Ehrenstorfer for providing the synthetic astaxanthin standard, as well as Dr Martin How, Dr Richard Webb and Ms Robyn Webb for help with preparation of the manuscript.

FUNDING

Funding of this work was provided by US Air Force Office of Scientific Research (AFOSR FA9550-09-1-0149), Asian Office of Aerospace Research and Development (AOARD-094073), the US National Science Foundation (NSF IOS0721608) and the Australian Research Council.

REFERENCES

Boal, J., Shashar, N., Grable, M., Vaughan, K., Loew, E. and Hanlon, R. (2004). Behavioral evidence for intraspecific signaling with achromatic and polarized light by cuttlefish (Mollusca: Cephalopoda). *Behaviour* **141**, 837-861.

Chayen, N. E., Cianci, M., Grossmann, J. G., Habash, J., Helliwell, J. R., Nneji, G. A., Raftery, J., Rizkallah, P. J. and Zagalsky, P. F. (2003). Unravelling the structural chemistry of the colouration mechanism in lobster shell. *Acta Crystallogr. D* **59**, 2072-2082.

Chiou, T.-H., Cronin, T. W., Caldwell, R. L. and Marshall, J. (2005). Biological polarized light reflectors in stomatopod crustaceans. *Proc. SPIE* **5888**, 380-388.

Chiou, T.-H., Mathger, L. M., Hanlon, R. T. and Cronin, T. W. (2007). Spectral and spatial properties of polarized light reflections from the arms of squid (*Loligo pealeii*) and cuttlefish (*Sepia officinalis* L.). *J. Exp. Biol.* **210**, 3624-3635.

Chiou, T.-H., Kleinlogel, S., Cronin, T., Caldwell, R., Loeffler, B., Siddiqi, A., Goldizen, A. and Marshall, J. (2008). Circular polarization vision in a stomatopod crustacean. *Curr. Biol.* **18**, 429-434.

Chiou, T. H., Marshall, N. J., Caldwell, R. L. and Cronin, T. W. (2011). Changes in light-reflecting properties of signalling appendages alter mate choice behaviour in a stomatopod crustacean *Haptosquilla trispinosa. Marine Freshw. Behav. Physiol.* **44**, 1-11.

Cronin, T. W., Shashar, N., Caldwell, R. L., Marshall, J., Cheroske, A. G. and Chiou, T.-H. (2003a). Polarization signals in the marine environment. *Proc. SPIE* **5158**, 85-92.

Cronin, T. W., Shashar, N., Caldwell, R. L., Marshall, J., Cheroske, A. G. and Chiou, T.-H. (2003b). Polarization vision and its role in biological signalling. *Integr. Comp. Biol.* **43**, 549-558.

Denton, E. J. F. R. S. and Nicol, J. A. C. (1965). Polarization of light reflected from the silvery exterior of the bleak, *Alburnus alburnus. J. Marine Biol. Assoc. UK* **45**, 705-709.

Dolan, P. M., Miller, D., Cogdell, R. J., Birge, R. R. and Frank, H. A. (2001). Linear dichroism and the transition dipole moment orientation of the carotenoid in the lh2

antenna complex in membranes of Rhodopseudomonas acidophila strain 10050. *J. Phys. Chem. B* **105**, 12134-12142.
Feynman, R. P., Leighton, R. B. and Sands, M. (1963). *The Feynman Lectures on Physics, 1, Mainly Mechanics, Radiation, and Heat*. Reading, Massachusetts: Addison-Wesley Publishing Company.
GoodWin, T. W. (1954). *Carotenoids, Their Comparative Biochemistry*. New York: Chemical Publishing Co. Inc.
Goodwin, T. and Srisukh, S. (1949). Some observations on astaxanthin distribution in marine Crustacea. *Biochem. J.* **45**, 268-270.
Grewe, C., Menge, S. and Griehl, C. (2007). Enantioselective separation of all-E-astaxanthin and its determination in microbial sources. *J. Chromatogr. A* **1166**, 97-100.
Gruszecki, W. I. (2004). Carotenoid orientation: role in membrane stabilization. In *Carotenoids in Health and Disease* (ed. N. I. Krinsky, S. T. Mayne and H. Sies), pp. 151-163. New York: Marcel Dekker.
Hofrichter, J. and Eaton, W. A. (1976). Linear dichroism of biological chromophores. *Annu. Rev. Biophys. Bioeng.* **5**, 511-560.
Horvath, G. and Varju, D. (2003). *Polarized Light in Animal Vision: Polarization Patterns in Nature*. Berlin Heidelberg: Springer-Verlag.
Laughlin, S., Menzel, R. and Snyder, A. W. (1975). Membranes, dichroism and receptor sensitivity. In *Photoreceptor Optics* (ed. A. W. Snyder and R. Menzel), pp. 237-259. New York, Heidelberg, Berlin: Springer-Verlag.
Margulies, L., Friedman, N., Sheves, M., Mazur, Y., Lippitsch, M. E., Riegler, M. and Aussenegg, F. R. (1985). Linear dichroism study of retinoids. *Tetrahedron* **41**, 191-195.
Marshall, N. J., Cronin, T. W., Shashar, N. and Land, M. (1999). Behavioural evidence for polarisation vision in stomatopods reveals a potential channel for communication. *Curr. Biol.* **9**, 755-758.
Mäthger, L. M. and Hanlon, R. T. (2006). Anatomical basis for camouflaged polarized light communication in squid. *Biol. Lett.* **2**, 494-496.
Matsuno, T., Maoka, T., Katsuyama, M., Ookubo, M., Katagiri, K. and Jimura, M. (1984). The occurrence of enantimomeric and meso-astaxanthin in aquatic animals. *Bull. Japan. Soc. Scient. Fish.* **50**, 1589-1592.
Okano, T., Fukada, Y. and Yoshizawa, T. (1995). Molecular basis for tetrachromatic color vision. *Comp. Biochem. Physiol.* **112B**, 405-414.
Parker, A. R. (2000). 515 million years of structural colour. *J. Opt. A* **2**, R15-R28.
Reynolds, E. S. (1963). The use of lead citrate at high pH as an electron-opaque stain in electron microscopy. *J. Cell Biol.* **17**, 208-212.
Rossel, S. (1989). Polarization sensitivity in compound eyes. In *Facets of Vision* (ed. D. G. Stavenga and R. C. Hardie), pp. 298-316. Berlin, Heidelberg: Springer-Verlag.
Shurcliff, W. and Ballard, S. (1964). *Polarized Light.* Princeton, New Jersey: D. Van Nostrand Company, Inc.
Snyder, A. W. and Laughlin, S. B. (1975). Dichroism and absorption by photoreceptors. *J. Comp. Physiol.* **100**, 101-116.
Sperling, W. and Rafferty, C. N. (1969). Relationship between Absorption spectrum and molecular conformations of 11-cis-retinal. *Nature* **224**, 591-594.
Sujak, A., Gabrielska, J., Milanowska, J., Mazurek, P., Strzalka, K. and Gruszeeki, W. I. (2005). Studies on canthaxanthin in lipid membranes. *Biochim. Biophys. Acta Biomembr.* **1712**, 17-28.
Sweeney, A., Jiggins, C. and Johnsen, S. (2003). Brief communication: polarized light as a butterfly mating signal. *Nature* **423**, 31-32.
Wolff, L. B. and Andreou, A. G. (1995). Polarization camera sensors. *Image Vision Comput.* **13**, 497-510.
Yoshizawa, T. (1994). Molecular basis for color vision. *Biophys. Chem.* **50**, 17-24.
Zagalsky, P., Eliopoulos, E. and Findlay, J. (1990). The architecture of invertebrate carotenoproteins. *Comp. Biochem. Physiol.* **97B**, 1-18.